Correspondence

Cramér–Rao Lower Bound Analysis for Elliptic Localization With Random Sensor Placements

Elliptic localization (EL) based on time-sum-of-arrival (TSOA) measurements has become popular due to its widespread applications in wireless sensor networks (WSNs) and distributed radar systems. While the performance limit of EL characterized by the Cramér–Rao lower bound (CRLB) has been thoroughly studied in literature when the sensor [transmitter and receiver (Rx)] positions are modeled as fixed deterministic quantities, the bound in the random network scenario has not been studied. This article introduces a methodology to investigate the TSOA-based localization performance, for the scenario where the sensors are randomly placed having their positions modeled by random parameters with their probability density functions specified. A tractable expression of the metric that approximates the CRLB and its distribution is analytically derived to characterize the fundamental limits of TSOA-based localization, which can be applied to both conventional WSNs and the special case in which the Rxs form a uniform linear array. Simulation results validate the theoretical development and demonstrate how the performance of EL is affected by the randomness of the sensor positions and different network parameters.

I. INTRODUCTION

Positioning using radar technologies has been extensively studied over the past few decades. Accurate location information enables numerous commercial and defense applications, including tracking, surveillance, autonomous driving, simultaneous localization and mapping, and so on [1]. The localization performance is governed by the accuracy of the location-related measurements, and unreliable measurements can limit the user experience of location-based services. Recent advancements in distributed multiple-input–multiple-output [2] and passive [3]

Manuscript received 16 July 2023; revised 3 November 2023 and 9 February 2024; accepted 17 February 2024. Date of publication 27 February 2024; date of current version 9 August 2024.

DOI. No. 10.1109/TAES.2024.3370890

Refereeing of this contribution was handled by O. Straka.

This work was supported in part by the Early Career Scheme (ECS) under Project 21205021 and the General Research Fund (GRF) under Project 11211122, both established under the University Grant Committee (UGC) of the Hong Kong Special Administrative Region, China, and in part by the City University of Hong Kong (CityU) under Project 7020083, and Project 7006090.

Authors' addresses: Jiajun He, Hing Cheung So, and Young Jin Chun are with the Department of Electrical Engineering, City University of Hong Kong, Hong Kong, China, E-mail: (jiajunhe5-c@my.cityu.edu.hk; hcso@ee.cityu.edu.hk; yjchun@cityu.edu.hk). Dominic K. C. Ho is with the Department of Electrical Engineering and Computer Science, University of Missouri, Columbia, MO 65211 USA, E-mail: (hod@missouri.edu). Wenxin Xiong is with the Department of Computer Science, University of Freiburg, Freiburg 79110, Germany E-mail: (w.x.xiong@outlook.com). *(Corresponding author: Young Jin Chun.)*

radar sensing technologies have enabled the acquisitions of high-accuracy time delay and arrival angle with a resolution of 3–30-cm spatial resolution and $< 1^\circ$, paving the way for the development of centimeter-level applications. Furthermore, the placement of transmitters (Txs) and receivers (Rxs) is critical for localization, where inadequate configurations can significantly impair localization accuracy.

Compared with circular positioning by time-of-arrival (TOA) [4] and hyperbolic positioning by time-difference-of-arrival (TDOA) [5], elliptic localization (EL) has been widely adopted in radar and sonar systems, multistatic arrays, and wireless positioning due to its higher flexibility and better accuracy control [6], [7]. Specifically, EL is an active approach to locate an object by the time-sum-of-arrival (TSOA) measurements from several Txs to the Rxs through the reflection by the object, where the trace of all possible reflection points from the measurement of a Tx–Rx pair forms an ellipse in the case of 2-D (ellipsoid for 3-D) [7]. In real-world scenarios, it may be challenging to use multiple Txs, and often one Tx is used instead. In such a case, it is necessary to have at least three Rxs in order to determine the object's location without ambiguity in 2-D [8].

Numerous localization algorithms have been proposed to locate an object using TSOAs when the Tx and Rx locations are known, and their performance is commonly assessed by comparison with the Cramér–Rao lower bound (CRLB), where [1] gives the standard procedure for its evaluation. When the Tx is moving and its position and velocity are unknown, a semidefinite relaxation method was developed in [9] to jointly estimate the object and Tx locations, along with the associated CRLB. A comprehensive analysis of TSOA-based localization was performed in [7], including an evaluation of the CRLB for EL under different synchronization conditions and a tractable expression for the optimal CRLB with the associated optimal Tx and Rx placement derived. However, these CRLBs were obtained assuming that the Tx and Rx positions are fixed deterministic quantities, making them unsuitable for scenarios where the Tx or Rx positions are better modeled as random parameters.

To characterize the range-based localization performance with random sensor positions, the authors in [10] approximated the CRLB for TOA-based localization by using the second-largest internodal angle and derived the distribution under random network settings. An accurate CRLB approximation method was introduced in [11] to derive the distribution of CRLB for TDOA-based localization under random network geometries, where the TDOAs are observed with respect to (w.r.t.) one reference sensor. However, this method does not support localization by the full set of TDOA measurements [12], where we have TDOAs for all sensor pairs. Furthermore, the approximation methods in [10] and [11] are only suitable for evaluating the localization performance under wireless sensor networks (WSNs) and cannot be applied to bistatic radar configurations. To the best of our knowledge, the CRLB analysis for EL with random sensor positions is still an open problem that has not been addressed.

Motivated by these limitations of the previous works, we shift our focus to TSOA-based localization and deduce the corresponding CRLB, where the positions of Txs and Rxs are random and characterized by their probability density functions (PDFs). The development in this work results in a tractable expression of the bound to assess the performance limit for both WSNs and bistatic radar configurations without resorting to time-consuming and complicated simulations. The main contributions of this article are summarized as follows.

1) *Tractable CRLB:* A performance bound that approximates the CRLB under white Gaussian noise for EL is developed, which unifies two different localization scenarios: 1) WSNs and 2) bistatic radar configurations. This bound is simple to evaluate, and simulation results show that it approaches the actual CRLB accurately.
2) *CRLB Distribution:* The distribution of the CRLB under white Gaussian noise for TSOA-based localization is derived analytically in terms of the spatial distribution of sensor nodes. It provides insight into the average localization performance when the sensor positions are random quantities.

The rest of this article is organized as follows. The system model is formulated in Section II. The state-of-the-art (SOTA) CRLB computation methods involving random parameters are introduced in Section III, and the proposed performance bound is derived in Section IV. Section V presents the simulations for validation. Finally, Section VI concludes this aticle.

II. SYSTEM MODEL

We consider a 2-D static EL system with one Tx and multiple Rxs, as described in [7]. Our goal is to determine the location of an object, denoted by $\boldsymbol{\psi} = [x, y]^T$, using time measurements. Two different EL scenarios are considered, namely, the WSN and a bistatic radar configuration. Fig. 1(a) depicts the TSOA-based localization in a typical WSN with L sensors. One sensor at position $\boldsymbol{\psi}_t = [x_t, y_t]^T$ acts as the Tx, while the remaining sensors are Rxs with positions $\boldsymbol{\psi}_l = [x_l, y_l]^T$, $l = 2, \ldots, L$. The Euclidean distance between the object and the lth sensor is given by: $d_l = \|\boldsymbol{\psi}_l - \boldsymbol{\psi}\|$. In practice, not all $L-1$ receiving sensors are available for localization due to the bandwidth and transmit power limits. We introduce a variable a_l to indicate the availability of sensor l, where $a_l = 1$ with probability $1 - p_a$. The number of participating sensors in the localization process is then equal to $\hat{L} = \sum_{l=1}^{L} a_l$. In a bistatic radar configuration, it is common for the Tx to have one omnidirectional antenna and for the Rxs to be the $\hat{L} - 1$ antenna elements of a uniform linear array (ULA) with interelement spacing λ, as illustrated in Fig. 1(b). This scenario is treated as a special case of a WSN where all Rxs form a ULA.

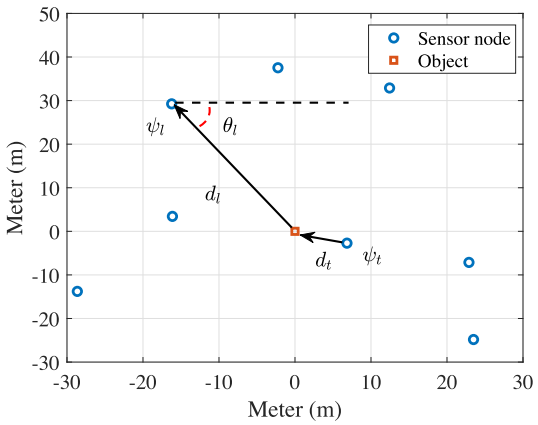

(a)

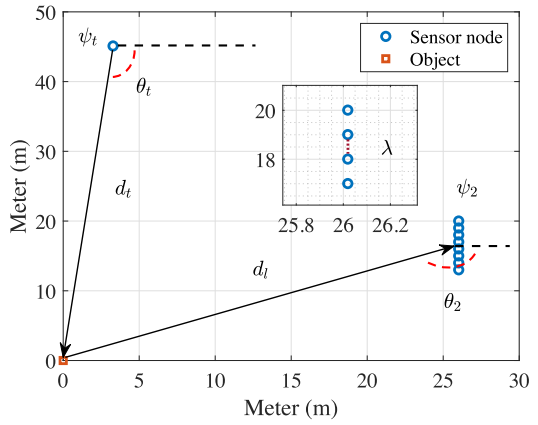

(b)

Fig. 1. Illustration of localization system model. (a) WSN. (b) Special case.

To account for the randomness of the sensor positions that often occur in practice, we do not assume the sensor positions $\boldsymbol{\psi}_t$ and $\boldsymbol{\psi}_l$ are known. Instead, they are modeled as unknown random parameters sampled from known spatial distributions $f(\boldsymbol{\psi}_t)$ and $f(\boldsymbol{\psi}_l)$. Various spatial distributions can be applied to model the randomness of the sensor locations, including the Gaussian and uniform distributions, which are widely utilized to simulate the user hotspot in heterogeneous networks [13]. The distance associated with the TSOA from the Tx through the object to the lth Rx is modeled as

$$r_l = \|\boldsymbol{\psi}_l - \boldsymbol{\psi}\| + \|\boldsymbol{\psi} - \boldsymbol{\psi}_t\| + n_l = d_l + d_t + n_l \quad (1)$$

where n_l is the zero-mean additive white Gaussian noise with known variance σ_n^2 [7].[1] The vector form of (1) is $\boldsymbol{r} = \boldsymbol{g}(\boldsymbol{\psi}) + \boldsymbol{n}$, where $\boldsymbol{r} = [r_2, r_3, \ldots, r_{\hat{L}}]^T$, $\boldsymbol{g}(\boldsymbol{\psi}) = [g_2(\boldsymbol{\psi}), g_3(\boldsymbol{\psi}), \ldots, g_{\hat{L}}(\boldsymbol{\psi})]^T$, and $\boldsymbol{n} = [n_2, n_3, \ldots, n_{\hat{L}}]^T$. In this article, our primary focus is on investigating the CRLB for TSOA-based localization under random sensor placement. For the estimators to determine the object location using TSOAs, see [7], [8], and [9].

[1]The nonline-of-sight condition is modeled by using a large value of σ_n^2.

III. CRLB ANALYSIS IN RANDOM WIRELESS NETWORKS

The CRLB is a commonly used metric for evaluating the performance of an unbiased estimator [1]. The CRLB that bounds the mean-square error (mse) for TSOA positioning is the trace of the inverse of the Fisher information matrix (FIM)

$$\text{CRLB(TSOA)} = \text{tr}(\text{FIM}^{-1}(\text{TSOA})) \quad (2)$$

$$\text{FIM(TSOA)} = \mathbb{E}\left\{-\frac{\partial^2 \ln f(\boldsymbol{r}; \boldsymbol{\psi})}{\partial \boldsymbol{\psi} \partial \boldsymbol{\psi}^T}\right\} \quad (3)$$

where $f(\boldsymbol{r}; \boldsymbol{\psi})$ represents the PDF of the TSOA measurement vector parameterized by the object location. Conventional approaches for computing the CRLB typically assume that the sensor (Tx and Rx) positions are fixed and deterministic. Next, we will introduce three SOTA approaches for analyzing this metric in random network settings, where sensor positions are treated as random parameters.

A. Numerical Computation

Numerical computation of the CRLB based on (2) requires the PDF of the TSOA vector parameterized only by the object position. Assuming that $\hat{L}$ sensors are available for localization, such a PDF can be obtained through marginalization by representing the joint PDF as conditional

$$f(\boldsymbol{r}; \boldsymbol{\psi}) = \int_{\boldsymbol{\psi}_t} \cdots \int_{\boldsymbol{\psi}_{\hat{L}}} f(\boldsymbol{\psi}_t, \boldsymbol{\psi}_2, \ldots, \boldsymbol{\psi}_{\hat{L}}) f(\boldsymbol{r}|\boldsymbol{\psi}_t, \boldsymbol{\psi}_2, \ldots, \boldsymbol{\psi}_{\hat{L}}) d\boldsymbol{\psi}_t d\boldsymbol{\psi}_2 \cdots d\boldsymbol{\psi}_{\hat{L}}. \quad (4)$$

Since the measurement noise is assumed to be independently and identically distributed (IID) with a zero-mean Gaussian distribution, i.e., $n_l \sim (0, \sigma_n^2)$, the PDF of the TSOA vector conditioned on Tx and Rx locations is

$$f(\boldsymbol{r}|\boldsymbol{\psi}_t, \boldsymbol{\psi}_2, \ldots, \boldsymbol{\psi}_{\hat{L}}) = \left(\frac{1}{\sqrt{2\pi}\sigma_n}\right)^{\hat{L}-1} \exp\left\{\frac{-1}{2\sigma_n^2} \sum_{l=2}^{\hat{L}} (r_l - d_l - d_t)^2\right\}. \quad (5)$$

When we model the spatial distribution of each sensor to be Gaussian and independent of the others, we have

$$f(\boldsymbol{\psi}_t, \boldsymbol{\psi}_2, \ldots, \boldsymbol{\psi}_{\hat{L}}) = \prod_{l=1}^{\hat{L}} \left(\frac{1}{\sqrt{2\pi}\sigma_l}\right)^2 \times \exp\left\{\frac{-1}{2\sigma_l^2}\left[(x_l - \bar{x}_l)^2 + (y_l - \bar{y}_l)^2\right]\right\} \quad (6)$$

where σ_l^2 is the variance of sensor node distribution and $(\bar{x}_l, \bar{y}_l)$ represents the mean of the lth sensor location in the Cartesian coordinates. Analytical evaluation of (4) with (5)–(6) is intractable. However, (4) can be evaluated numerically [14], and the associated CRLB, denoted by CRLB_{nc}(TSOA), can be calculated by (2)–(3). For other

sensor spatial distributions, (4) and (5) still apply, and (6) should be updated accordingly.

REMARK 1 This method does not provide a closed-form expression of (2), making it difficult to understand how the randomness of the sensor positions affects the localization performance. However, the result can align with the actual CRLB. See [15] for the details of evaluating the CRLB using numerical computation.

B. Modified CRLB

The modified CRLB can provide the performance limit of an estimation problem, which has been utilized for analyzing the estimation performance in the presence of Rayleigh fading [16]. It removes the randomness of the sensor positions by taking the expectation over them in the FIM to generate

$$\begin{aligned}&\mathbb{E}_{\boldsymbol{n},\boldsymbol{\rho}}\left[-\frac{\partial^2 \ln f(\boldsymbol{r},\boldsymbol{\rho};\boldsymbol{\psi})}{\partial\boldsymbol{\psi}\partial\boldsymbol{\psi}^T}\right]\\&=\mathbb{E}_{\boldsymbol{\rho}}\left\{\mathbb{E}_{\boldsymbol{n}|\boldsymbol{\rho}}\left[\text{FIM(TSOA}|\boldsymbol{\rho})\right]\right\}\end{aligned}\tag{7}$$

where $\boldsymbol{\rho}=\{\boldsymbol{\psi}_t,\boldsymbol{\psi}_2,\ldots,\boldsymbol{\psi}_{\hat{L}}\}$. The modified CRLB of the object position is then given by

$$\begin{aligned}&\text{CRLB}_{\text{m}}\text{(TSOA)}\\&=\text{tr}\left(\left[\mathbb{E}_{\boldsymbol{\rho}}\left\{\mathbb{E}_{\boldsymbol{n}|\boldsymbol{\rho}}\left[\text{FIM(TSOA}|\boldsymbol{\rho})\right]\right\}\right]^{-1}\right).\end{aligned}\tag{8}$$

REMARK 2 The modified CRLB is computed by taking the expected value of FIM over the sensor positions, indicating that (8) is not equivalent to the exact CRLB obtained by (2) due to the fact $1/\mathbb{E}[x]\neq\mathbb{E}[1/x]$. The modified CRLB is found to be quite lower than the exact CRLB in the problem considered and will not be discussed further.

C. Approximate CRLB

An alternative approach is to approximate the CRLB in (2) by characterizing it as a function of a single random variable ((r. v.)) Θ [10], [11], and we denote this bound by $\text{CRLB}_{\text{a}}\text{(TSOA)}$. When the distribution of Θ is known, we can evaluate the probability $P(\text{CRLB}_{\text{a}}\text{(TSOA)}\leq s)$, where s is the given localization accuracy, e.g., 1 m^2. Based on this idea, we derive the CRLB distribution for TSOA-based positioning in the following section.

IV. UNIFIED CRLB IN RANDOM NETWORKS

A. WSN Localization

Let us assume that the locations of the sensors are given *a priori* and the FIM for the object position $\boldsymbol{\psi}$ under Gaussian measurement noise is [1]

$$\text{FIM(TSOA)}=\left[\frac{\partial\boldsymbol{g}(\boldsymbol{\psi})}{\partial\boldsymbol{\psi}}\right]^T\boldsymbol{C}^{-1}\left[\frac{\partial\boldsymbol{g}(\boldsymbol{\psi})}{\partial\boldsymbol{\psi}}\right]\tag{9}$$

where $\boldsymbol{C}$ is the measurement covariance matrix equal to $\sigma_n^2\cdot\mathbf{I}$ in our case. Let θ_t be the azimuth angle of the object w.r.t. the Tx and θ_l be that viewed from Rx l, as illustrated in Fig. 1. The partial derivative of $\boldsymbol{g}(\boldsymbol{\psi})$ w.r.t. $\boldsymbol{\psi}$ is

$$\begin{aligned}\frac{\partial\boldsymbol{g}(\boldsymbol{\psi})}{\partial\boldsymbol{\psi}}&=\begin{bmatrix}\frac{x-x_2}{d_2}+\frac{x-x_t}{d_t} & \frac{y-y_2}{d_2}+\frac{y-y_t}{d_t}\\ \vdots & \vdots\\ \frac{x-x_{\hat{L}}}{d_{\hat{L}}}+\frac{x-x_t}{d_t} & \frac{y-y_{\hat{L}}}{d_{\hat{L}}}+\frac{y-y_t}{d_t}\end{bmatrix}\\&=\begin{bmatrix}\cos\theta_2+\cos\theta_t & \sin\theta_2+\sin\theta_t\\ \vdots & \vdots\\ \cos\theta_{\hat{L}}+\cos\theta_t & \sin\theta_{\hat{L}}+\sin\theta_t\end{bmatrix}.\end{aligned}\tag{10}$$

By substituting (10) into (9), we have

$$\text{FIM(TSOA)}=\frac{1}{\sigma_n^2}\cdot\begin{bmatrix}f_1 & f_2\\ f_2 & f_3\end{bmatrix}\tag{11}$$

where

$$\begin{aligned}f_1&=\sum_{l=2}^{\hat{L}}(\cos\theta_l+\cos\theta_t)^2\\f_2&=\sum_{l=2}^{\hat{L}}(\sin\theta_l+\sin\theta_t)(\cos\theta_l+\cos\theta_t)\\f_3&=\sum_{l=2}^{\hat{L}}(\sin\theta_l+\sin\theta_t)^2.\end{aligned}\tag{12}$$

The CRLB for the object position $\boldsymbol{\psi}$ based on TSOA measurements, as shown in (2), is then computed by

$$\text{CRLB(TSOA)}=\text{tr}\left(\text{FIM}^{-1}\text{(TSOA)}\right)=\sigma_n^2\cdot\frac{b}{D}\tag{13}$$

where

$$\begin{aligned}b&=\sum_{l=2}^{\hat{L}}(\cos\theta_l+\cos\theta_t)^2+(\sin\theta_l+\sin\theta_t)^2\\&=\sum_{l=2}^{\hat{L}}\cos^2\theta_l+\cos^2\theta_t+2\cos\theta_l\cos\theta_t\\&\quad+\sin^2\theta_l+\sin^2\theta_t+2\sin\theta_l\sin\theta_t\\&=\sum_{l=2}^{\hat{L}}2+2\left(\cos\theta_l\cos\theta_t+\sin\theta_l\sin\theta_t\right)\\&=\sum_{l=2}^{\hat{L}}2+2\cos(\theta_l-\theta_t)\leq 4(\hat{L}-1).\end{aligned}\tag{14}$$

Then, we approximate the denominator of the CRLB D in (13) as

$$\begin{aligned}D=&\sum_{l=2}^{\hat{L}}(\cos\theta_l+\cos\theta_t)^2\sum_{l=2}^{\hat{L}}(\sin\theta_l+\sin\theta_t)^2\\&-\left(\sum_{l=2}^{\hat{L}}(\cos\theta_l+\cos\theta_t)(\sin\theta_l+\sin\theta_t)\right)^2\end{aligned}$$

$$\overset{(a)}{\approx} \sum_{l=2}^{\hat{L}} (\cos\theta_l + \cos\theta_t)^2 \sum_{l=2}^{\hat{L}} (\sin\theta_l + \sin\theta_t)^2$$
$$\overset{(b)}{\approx} \sum_{l=2}^{\hat{L}} (\cos\theta_l + 1)^2 \sum_{l=2}^{\hat{L}} \sin^2\theta_l$$
$$\overset{(c)}{\leq} (\hat{L}-1) \sum_{l=2}^{\hat{L}} (\cos\theta_l + 1)^2 \tag{15}$$

where $\left(\sum_{l=2}^{\hat{L}} (\cos\theta_l + \cos\theta_t)(\sin\theta_l + \sin\theta_t)\right)^2$ was neglected in (a) when there are sufficient number of sensors [11], which has also been verified by [10] via simulation. (b) is achieved by choosing the coordinate reference with the object as the origin and the Tx on the positive x-axis such that $\cos\theta_t = 1, \sin\theta_t = 0$ [7], and (c) sets $\sum_{l=2}^{\hat{L}} \sin^2\theta_l$ to its maximum value, i.e., $(\hat{L}-1)$. Utilizing the CRLB in (13) by taking the maximum values of b and D in (14)–(15) leads to the approximate CRLB of the object position

$$\text{CRLB}_{\text{a}}(\text{TSOA}) \approx \sigma_n^2 \cdot \frac{4}{\sum_{l=2}^{\hat{L}} (\cos\theta_l + 1)^2}. \tag{16}$$

However, it is still hard to derive the CRLB distribution as (16) contains the summation of the terms $(\cos\theta_l + 1)^2$.

To approximate the CRLB using a single (r. v.) based on the notion of mutual information [10] that is commonly used in machine learning and statistics, we can select a $\Theta \in \{\theta_l\}_{l=2}^{\hat{L}}$ that provides the highest amount of information to the denominator of (13) through maximizing the mutual information. The mutual information is

$$I\left(D; \theta_l | \hat{L}\right) = h\left(D|\hat{L}\right) - h\left(D|\theta_l, \hat{L}\right) \tag{17}$$

and the differential entropies are given by

$$\begin{aligned} h(D|\hat{L}) = & -\int_{\bar{\text{D}}} f_D(d|\hat{L}) \log_2 f_D(d|\hat{L}) \text{d}d \\ h(D|\theta_l, \hat{L}) = & -\int_{\bar{\text{D}}} \int_{\bar{\theta}} f_{D;\theta_l}(d, \theta_l|\hat{L}) \\ & \times \log_2 f_D(d|\theta_l, \hat{L}) \text{d}d\text{d}\theta_l \end{aligned} \tag{18}$$

where $f_D(\cdot)$ and $f_{D;\theta_l}(\cdot)$ represent the PDF of D and the joint PDF of D and θ_l, respectively. $\bar{\text{D}}$ and $\bar{\theta}$ denote the supports of d and θ_l. These PDFs can be obtained through Monte Carlo simulations. Based on the selected Θ, the denominator of (16) is rewritten as

$$D_a \approx (\hat{L}-1)(\cos\Theta + 1)^2. \tag{19}$$

To conclude, we have the following corollary.

COROLLARY 1 Assuming that $\hat{L}$ sensors are detected and choosing the angle $\theta_t = 0$ for the reference purpose, there exists a $\Theta \in \{\theta_l\}_{l=2}^{\hat{L}}$ that provides the highest amount of information in terms of mutual information among the $\hat{L}-1$ Rxs such that the CRLB of the object position from TSOA measurements with white Gaussian noise of power σ_n^2 can be approximated by

$$\text{CRLB}_{\text{a}}(\text{TSOA}) \approx \sigma_n^2 \cdot \frac{4}{(\hat{L}-1)(\cos\Theta + 1)^2} \tag{20}$$

where the value of Θ is related to the spatial distribution of the sensors.

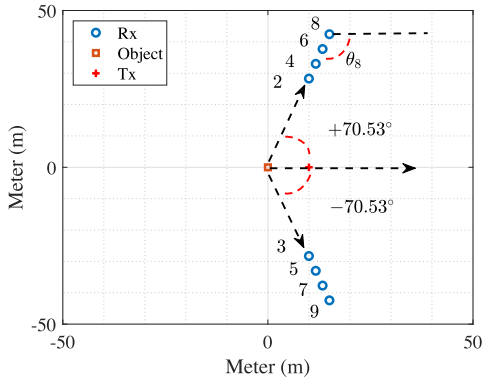

Fig. 2. Optimal sensor placement according to A-optimality for localization of an object with one Tx and eight Rxs ($\hat{L} = 9$), where half of the Rxs are placed along the straight line with an angle of 70.53° w.r.t. the object above the axis defined by the object and Tx positions and the other half below [7].

REMARK 3 From the derivations in [7] by invoking the Courant–Fischer–Weyl min-max principle [17] and selecting a coordinate reference as step (15.b), the optimal sensor placement by the A-optimality that minimizes the trace of the CRLB matrix (2) is achieved when the FIM (9) is diagonal [7], i.e.,

$$\sum_{l=2}^{\hat{L}} \sin\theta_l (\cos\theta_l + 1) = 0 \tag{21}$$

and a tractable expression of the A-optimal CRLB for the deterministic scenario is [7]

$$CRLB_{\text{o}}(TSOA) \approx \sigma_n^2 \cdot \frac{27}{16\hat{L}}. \tag{22}$$

By having odd $\hat{L}$, $\theta_t = 0$, and $\theta_l = -\theta_{l+1}$, where $l = 2, 4, \ldots, \hat{L}-1$, the optimal sensor placement appears when $\cos\theta_l = -1/3$, i.e., $\theta_l \approx 180° - 70.53°$. Fig. 2 depicts the optimal sensor placement for EL when $\hat{L} = 9$, where the Tx is placed in the positive x-axis with the object at the origin and the Rxs are allocated along two straight lines having angles $\pm 70.53°$ with half of the Rxs in each. The Rxs with an angle of 70.53° are assigned even indexes, while the Rxs with an angle of $-70.53°$ are assigned odd indexes. For the optimal localization performance with two Txs, see [18] for the details.

For a particular interest in the CRLB with multiple Txs, we update Corollary 1 as follows. Considering N Txs and M Rxs are detected for use in a localization area, the CRLB in this case is

$$\text{CRLB}_t(\text{TSOA}) = \sigma_n^2 \cdot \frac{b_t}{D_t} \tag{23}$$

where

$$b_t = \sum_{m=1}^{M}\sum_{n=1}^{N}(\cos\theta_m + \cos\theta_{t,n})^2 + (\sin\theta_m + \sin\theta_{t,n})^2 \tag{24}$$

and

$$D_t = \sum_{m=1}^{M}\sum_{n=1}^{N}(\sin\theta_m + \sin\theta_{t,n})^2 \times \sum_{m=1}^{M}\sum_{n=1}^{N}(\cos\theta_m + \cos\theta_{t,n})^2 - \left(\sum_{m=1}^{M}\sum_{n=1}^{N}(\sin\theta_m + \sin\theta_{t,n}) \times (\cos\theta_m + \cos\theta_{t,n})\right)^2. \tag{25}$$

By applying similar steps in approximating b_t and D_t, as described in Corollary 1, we have

$$b_t \le 4MN, \text{ and } D_t \approx (MN)^2(\cos\Theta_t + 1)^2 \tag{26}$$

where Θ_t is the angle that contributes the highest amount of information to D_t in terms of mutual information among the sensors. Thus, the approximate CRLB of the object position is

$$\text{CRLB}_{\text{a},t}(\text{TSOA}) \approx \sigma_n^2 \cdot \frac{4}{MN(\cos\Theta_t + 1)^2}. \tag{27}$$

Alternatively, the denominator of (13) can be approximated, as described in [11]. We first rewrite (15) into

$$D \approx (\hat{L}-1)\sum_{l=2}^{\hat{L}}(\cos\theta_l + 1)^2 = (\hat{L}-1)\sum_{l=2}^{\hat{L}}(1 + 2\cos\theta_l + \cos^2\theta_l). \tag{28}$$

The approximation strategy replaces the term $\sum_{l=2}^{\hat{L}} 1 + \cos^2\theta_l$ with a proper constant, and thus, D will become a function of $\sum_{l=2}^{\hat{L}}\cos\theta_l$ only. By setting $\eta \triangleq \sum_{l=2}^{\hat{L}} 1 + \cos^2\theta_l$, we have

$$D \approx (\hat{L}-1)\sum_{l=2}^{\hat{L}}(1 + \cos^2\theta_l) + (\hat{L}-1)\sum_{l=2}^{\hat{L}} 2\cos\theta_l = (\hat{L}-1)\cdot\eta + 2(\hat{L}-1)\sum_{l=2}^{\hat{L}}\cos\theta_l. \tag{29}$$

Let $\hat{D} = D/(\hat{L}-1) - 2\sum_{l=2}^{\hat{L}}\cos\theta_l$, we then define an l_p-norm minimization problem as

$$\hat{\eta} \to \arg\min_{\eta} f_p(\eta) = \arg\min_{\eta}\sum_{n=1}^{\mathcal{N}}\left|\hat{D}[n] - \eta\right|^p \tag{30}$$

where $1 \le p \le 2$, $\hat{D}[n]$ is the observation of $\hat{D}$ in the nth realization of the sensor positions, where $n = 1, 2, \ldots, \mathcal{N}$. Then, the compact matrix form of (30) is given by

$$\arg\min_{\eta} f_p(\eta) = \arg\min_{\eta}\|\boldsymbol{A}\eta - \boldsymbol{b}\|_p^p = \arg\min_{\eta}\|\boldsymbol{q}\|_p^p \tag{31}$$

where $\boldsymbol{A} = [1, \ldots, 1]^T$, $\boldsymbol{b} = [\hat{D}[1], \ldots, \hat{D}[\mathcal{N}]]^T$ and $\boldsymbol{q} = \boldsymbol{A}\eta - \boldsymbol{b} = [q[1], \ldots, q[\mathcal{N}]]^T$. We can rewrite (30) as

$$f_p(\eta) = \sum_{n=1}^{\mathcal{N}}|q_n|^p = \sum_{n=1}^{\mathcal{N}}|q_n|^{p-2}q_n^2 \tag{32}$$

and interpret $|q_n|^{p-2}$ to be the weight in each observation. η can then be obtained by using the iteratively reweighted least squares (IRLS) as [19]

$$\hat{\eta} = (\boldsymbol{A}^T\boldsymbol{W}\boldsymbol{A})^{-1}\boldsymbol{A}^T\boldsymbol{W}\boldsymbol{b} \tag{33}$$

where $\boldsymbol{W} = \text{diag}(|q_1|^{p-2}, |q_2|^{p-2}, \ldots, |q_N|^{p-2})$. In conclusion, we have the following corollary.

COROLLARY 2 Assume that $\hat{L}$ sensors are present for localization, there exists an $\hat{\eta}$ such that the CRLB of the object position in (2) with the FIM given by (9) can be approximated by

$$CRLB_{\text{a}}(TSOA) \approx \sigma_n^2 \cdot \frac{4}{\hat{\eta} + 2\Phi} \tag{34}$$

where $\Phi = \sum_{l=2}^{\hat{L}}\cos\theta_l$ and has a PDF given by [20]

$$f(\Phi \mid \hat{L}-1) = \frac{1}{2\pi}\int_{-\infty}^{\infty}\left[\frac{J_0(x)}{I_0(0)}\right]^{\hat{L}-1} e^{-i\Phi x}dx \tag{35}$$

where $I_0(\cdot)$ is the modified Bessel function of order zero and $J_0(\cdot)$ is the integral form of the zero-order Bessel function.

Corollary 2 indicates that the approximate CRLB is parameterized by $\sum_{l=2}^{\hat{L}}\cos\theta_l$. Given $\hat{L}$ and σ_n^2, its cumulative distribution can be obtained from that of Φ

$$\begin{aligned} &P(\text{CRLB}_{\text{a}}(\text{TSOA}) \le s \mid \sigma_n, \hat{L}, \hat{\eta}) \\ &= P\left(\sigma_n^2 \cdot \frac{4}{\hat{\eta} + 2\Phi} \le s \,\middle|\, \sigma_n, \hat{L}, \hat{\eta}\right) \\ &= P\left(\frac{4\sigma_n^2}{s} \le \hat{\eta} + 2\Phi \,\middle|\, \sigma_n, \hat{L}, \hat{\eta}\right) \\ &= 1 - P\left(\Phi \le \frac{2\sigma_n^2}{s} - \frac{\hat{\eta}}{2} \,\middle|\, \sigma_n, \hat{L}, \hat{\eta}\right). \end{aligned} \tag{36}$$

It is worth noting that the approximation method from [11], as described in Corollary 2, cannot be extended to the case with multiple Txs because the denominator of the CRLB contains a summation of cosine terms. The method provided in Corollary 1 addresses this limitation of [11] and opens the possibility of approximating the CRLB for localization with the full set of TDOA measurements.

B. Special Case

In the special case where all receiving sensors form a ULA, which often appears in the bistatic radar configuration, the performance of TSOA-based localization is

degraded due to the loss of one degree of freedom (DoF). In addition, it is evident that the denominator of (13) is approximately equal to zero when the interelement spacing of the ULA is sufficiently small, rendering Corollary 1 inadequate for characterizing its performance. Without applying the approximation in step (a), (15) becomes

$$\begin{aligned} D &= (\hat{L}-1)\sum_{l=2}^{\hat{L}}(\cos\theta_l+1)^2 \\ &\quad -\left(\sum_{l=2}^{\hat{L}}\sin\theta_l(\cos\theta_l+1)\right)^2 \\ &\overset{(d)}{\geq} (\hat{L}-1)\sum_{l=2}^{\hat{L}}(\cos\theta_l+1)^2 \\ &\quad -\sum_{l=2}^{\hat{L}}(\cos\theta_l+1)^2\sum_{l=2}^{\hat{L}}\sin^2\theta_l \\ &= \left[(\hat{L}-1)-\sum_{l=2}^{\hat{L}}\sin^2\theta_l\right]\cdot\sum_{l=2}^{\hat{L}}(\cos\theta_l+1)^2 \end{aligned} \tag{37}$$

where (d) follows from the Cauchy–Schwarz inequality. Thus, the approximate CRLB given by Corollary 1 can be rewritten as

$$\mathrm{CRLB_a(TSOA)} \approx \sigma_n^2\cdot\frac{4\epsilon}{(\hat{L}-1)(\cos\Theta+1)^2} \tag{38}$$

where $\epsilon = 1/\cos^2\Theta$. To represent the CRLB using a single (r. v.), ϵ is approximated using a suitable constant, as described in [11], and its estimate can be determined by solving

$$\begin{aligned} \hat{\epsilon} \rightarrow \arg\min_{\epsilon}\sum_{n=1}^{\mathcal{N}}\big(&\epsilon\cdot\mathrm{CRLB_a(TSOA)}[n] \\ &-\mathrm{CRLB(TSOA)}[n]\big)^2 \end{aligned} \tag{39}$$

where $\mathrm{CRLB_a(TSOA)}[n]$ and $\mathrm{CRLB(TSOA)}[n]$ are given by Corollary 1 and {(2), (9)} using different network configurations, respectively, and the optimization problem can be solved using the IRLS stated in (30) to (33) for a number of network configurations denoted by $\mathcal{N}$ in (39). The parameter ϵ is treated as a constant that is common across different network configurations [21] and therefore (39) needs to perform only once for a given $\hat{L}$. To summarize, we present the unified CRLB for both WSN and bistatic radar cases in the following proposition.

PROPOSITION 1 (Unified CRLB) Assuming that L sensors are present and $\hat{L} = \sum_{l=1}^{L} a_l$ sensors participate in localization, in which their positions are modeled as random parameters. There exists an $\hat{\epsilon}$ such that the performance lower bound of TSOA-based systems for locating an object under white Gaussian noise in WSNs or bistatic radar configurations is given by

$$\mathit{CRLB_a(TSOA)} \approx \sigma_n^2\cdot\frac{4\hat{\epsilon}}{(\hat{L}-1)(\cos\Theta+1)^2} \tag{40}$$

where $\Theta \in \{\theta_l\}_{l=2}^{\hat{L}}$ provides the highest amount of information among the sensors according to the mutual information computed by (17) and θ_l is the azimuth of the object w.r.t. Rx l such that the azimuth of the object w.r.t. the Tx is zero.

Note that Corollary 1 is a special case of Proposition 1 when $\hat{\epsilon} = 1$, and its performance can be improved by selecting a suitable $\hat{\epsilon}$. Compared with [11], Proposition 1 does not ignore the term $\left(\sum_{l=2}^{\hat{L}}\sin\theta_l(\cos\theta_l+1)\right)^2$ in (37), thereby leading to a better approximation accuracy. Proposition 1 indicates that the CRLB for TSOA localization is a function of σ_n^2, $\hat{L}$, and Θ. Given σ_n^2 and $\hat{L}$, the cumulative distribution of the CRLB on (2) can be obtained in terms of the cumulative distribution of Θ

$$\begin{aligned} &P(\mathrm{CRLB_a(TSOA)} \leq s \mid \sigma_n, \hat{L}, \hat{\epsilon}) \\ &= P\left(\sigma_n^2\cdot\frac{4\hat{\epsilon}}{(\hat{L}-1)(\cos\Theta+1)^2} \leq s \;\middle|\; \sigma_n, \hat{L}, \hat{\epsilon}\right) \\ &= P\left(\frac{4\sigma_n^2\hat{\epsilon}}{s} \leq (\hat{L}-1)(\cos\Theta+1)^2 \;\middle|\; \sigma_n, \hat{L}, \hat{\epsilon}\right) \\ &= 1-P\left(\Theta \leq \arccos\left(2\sigma_n\sqrt{\frac{\hat{\epsilon}}{s(\hat{L}-1)}}-1\right) \;\middle|\; \sigma_n, \hat{L}, \hat{\epsilon}\right) \end{aligned} \tag{41}$$

where s is the specified accuracy requirement in terms of the mse of a location estimate. The derived bound can provide insights to a system designer on how the network configurations can be adjusted to achieve the intended localization accuracy.

V. SIMULATION RESULTS

A. Simulation Setup

This section examines the accuracy of the bound defined by Proposition 1 and compares it with the actual CRLB obtained by the method introduced in Section III-A via 1×10^5 realizations at a certain noise level. The object is located at the origin $\boldsymbol{\psi} = [0, 0]^T$. The sensor locations are randomly generated from a uniform distribution within a circle centered at the origin with a radius of 50 m. For the special case where all receivers form a linear array, the array center is chosen by the same uniform distribution, and it is arranged vertically with an interelement spacing of $\lambda = 0.5$ m. In the case of WSN, we set $\hat{\epsilon} = 1$ in the simulations. However, for the bistatic radar configuration, the value of $\hat{\epsilon}$ is determined as 6 from (39) through $\mathcal{N} = 1\times10^6$ observations. The variance of the range error is set to $\sigma_n^2 = 1/(10^{\frac{\mathrm{SNR}}{10}})$ [7], where SNR is the signal-to-noise ratio in dB. During the simulation, the impact of the network load is ignored, i.e., $p_a = 0$, and its influence will be manifested by reducing the number of sensors.

B. Accuracy of the Bound by Proposition 1

Fig. 3 plots the accuracy of the approximate CRLB using Corollary 1 in the general WSN scenario. The obtained result is compared with the exact CRLB by (2) and the A-optimal CRLB [7] given by (22). It is observed that the

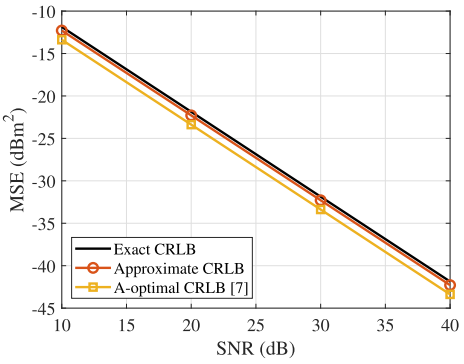

Fig. 3. Accuracy of approximate CRLB from Corollary 1 versus SNR for random sensor network when $L = 9$.

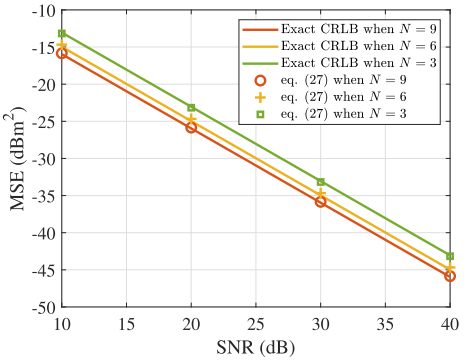

Fig. 4. Accuracy of approximate CRLB (27) of the multiple Tx case versus SNR for random sensor network when $M = 4$.

devised benchmark (20) is very close to the exact CRLB. If the fixed optimal sensor geometry is adopted, the localization error of TSOA-based localization decreases, resulting in a lower CRLB compared to the devised benchmark. Furthermore, Fig. 4 examines the approximate CRLB in (27) for the multiple Tx case. It is clear that the localization performance of EL increases with the number of Txs participating in localization. The approximate CRLBs, indicated by the green square, yellow plus sign, and red circle, closely follow the exact CRLBs represented by the solid green, yellow, and red lines, indicating that the approximation method described in Corollary 1 is not only suitable for the EL scenario with a single Tx but also applicable to the EL scenario involving multiple Txs, and the approximation error in Corollary 1 can be further decreased by optimizing $\hat{\epsilon}$.

In the special case of a linear arrangement of Rxs, the localization performance will greatly deteriorate as one DoF is lost from the collected TSOA measurements. Fig. 5 illustrates that the localization performance decreases in comparison to the result in Fig. 3, including the CRLB value obtained in WSNs and its A-optimal localization performance given by (22). It is seen that the approximation error between the bound from Corollary 1 and the exact CRLB increases significantly. By introducing the constant $\hat{\epsilon}$, it is shown that the approximate CRLB by Proposition 1 approaches the actual CRLB. It indicates that the proposed approximate bound not only characterizes the localization performance for TSOA-based positioning in conventional

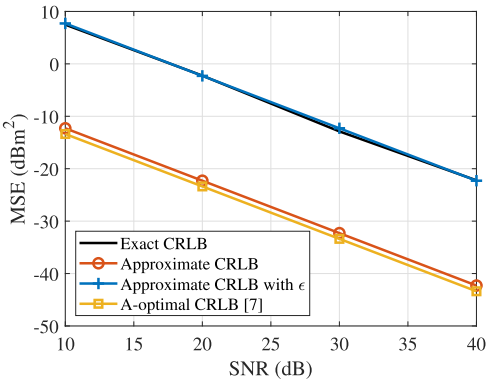

Fig. 5. Accuracy of approximate CRLB from Proposition 1 versus SNR for the special case of random placements of linear arrangement of Rxs when $L = 9$.

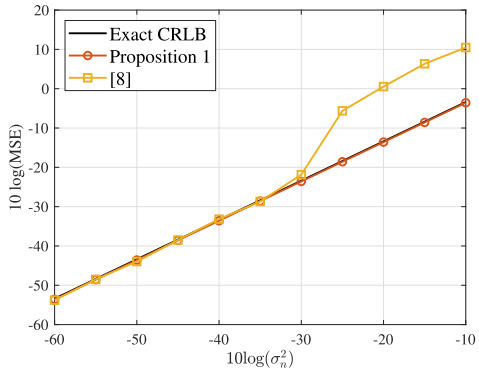

Fig. 6. Comparison between localization performance of [8] and approximate CRLB from Proposition 1.

WSNs but also in the special case of a linear array of Rxs that appear in bistatic radar localization.

C. Impact of Network Configurations on CRLB Distribution

We first examine the effectiveness of Proposition 1 by validating it with the localization performance of the positioning algorithm from [8] utilizing the same noise settings. It is observed in Fig. 6 that the mse of [8] reaches the CRLB under small noise conditions, and the developed approximate CRLB is very close to the actual CRLB, demonstrating the potential of leveraging a single (r. v.) to characterize the performance bound of TSOA-based localization. It supports that the devised benchmark can be applied to evaluate various TSOA positioning approaches with extremely high computational efficiency. Furthermore, we examine the accuracy of the CRLB distribution (41) in Fig. 7 by numerical evaluation of the probability with the uniformly generated sensor positions stated at the beginning of this section. It is seen that the devised CRLB cumulative distribution closely approximates the actual one from the exact CRLB, affirming the validity of (41). When σ_n is fixed at 5 m, the yellow, green, and blue curves in Fig. 7 show that the localization accuracy of TSOA positioning increases with the number of participating sensors L. Nevertheless, deploying a larger number of sensors also escalates the cost of the overall system. Hence, it is vital to strike a

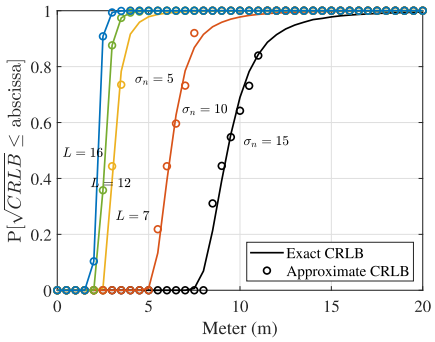

Fig. 7. Accuracy of approximate CRLB cumulative distribution versus the range error when $L = 7$ and the number of available sensors when $\sigma_n = 5$ m.

balance between the cost of a localization system and the desired positioning accuracy. Note that reducing the number of sensor nodes affects the network load on localization performance. Fig. 7 also evaluates the impact of the range error on the localization performance when $L = 7$. It indicates that the positioning error is more sensitive to σ_n than L, as demonstrated by yellow, red, and black curves. The proposed benchmark provides valuable insights for optimizing the network settings and configurations to meet the desired requirement of localization accuracy.

VI. CONCLUSION

This article derived a tractable expression that approximates the CRLB of TSOA-based localization together with its cumulative distribution, providing insights into the impact of random sensor placements on the localization accuracy. The approximate CRLB and the distribution accurately reflect the actual localization performance of both conventional WSNs and typical bistatic radar configurations. They can serve as valuable benchmarks for designers to evaluate the statistical average performance of a TSOA localization system under random sensor allocations without the need for lengthy and complex simulations.

JIAJUN HE, *Student Member, IEEE*
City University of Hong Kong, Hong Kong, China

DOMINIC K. C. HO, *Fellow, IEEE*
University of Missouri, Columbia, MO USA

WENXIN XIONG, *Graduate Student Member, IEEE*
University of Freiburg, Freiburg, Germany

HING CHEUNG SO, *Fellow, IEEE*
City University of Hong Kong, Hong Kong, China

YOUNG JIN CHUN, *Member, IEEE*
City University of Hong Kong, Hong Kong, China

REFERENCES

[1] H. C. So, "Source localization: Algorithms and analysis," in *Handbook of Position Location: Theory, Practice and Advances*, S. A. Zekavat and M. Buehrer, Eds., Piscataway, NJ, USA: Wiley-IEEE Press, 2019, ch. 3.

[2] L. Lan, M. Rosamilia, A. Aubry, A. De Maio, G. Liao, and J. Xu, "Adaptive target detection with polarimetric FDA-MIMO radar," *IEEE Trans. Aerosp. Electron. Syst.*, vol. 59, no. 3, pp. 2204–2220, Jun. 2023.

[3] G. Giunta, L. Pallotta, and D. Orlando, "Detecting sensor failures in TDOA-based passive radars: A statistical approach based on outlier distribution," *IEEE Trans. Aerosp. Electron. Syst.*, vol. 59, no. 3, pp. 2176–2187, Jun. 2023.

[4] K. W. Cheung, H. C. So, W. -K. Ma, and Y. T. Chan, "Least squares algorithms for time-of-arrival-based mobile location," *IEEE Trans. Signal Process.*, vol. 52, no. 4, pp. 1121–1130, Apr. 2004.

[5] Y. T. Chan and K. C. Ho, "A simple and efficient estimator for hyperbolic location," *IEEE Trans. Signal Process.*, vol. 42, no. 8, pp. 1905–1915, Aug. 1994.

[6] C.-W. Kiang and J.-F. Kiang, "Imaging on underwater moving targets with multistatic synthetic aperture sonar," *IEEE Trans. Geosci. Remote Sens.*, vol. 60, 2022, Art. no. 4211218.

[7] L. Rui and K. C. Ho, "Elliptic localization: Performance study and optimum receiver placement," *IEEE Trans. Signal Process.*, vol. 62, no. 18, pp. 4673–4688, Sep. 2014.

[8] S. S A. Al-Samahi, Y. Zhang, and K. C. Ho, "Elliptic and hyperbolic localizations using minimum measurement solutions," *Signal Process.*, vol. 167, 2020, Art. no. 107273.

[9] G. Wang, R. Zheng, and K. C. Ho, "Elliptic localization of a moving object by transmitter at unknown position and velocity: A semidefinite relaxation approach," *IEEE Trans. Mobile Comput.*, vol. 22, no. 5, pp. 2675–2692, May 2023.

[10] C. E. O'Lone, H. S. Dhillon, and R. M. Buehrer, "A statistical characterization of localization performance in wireless networks," *IEEE Trans. Wireless Commun.*, vol. 17, no. 9, pp. 5841–5856, Sep. 2018.

[11] J. He, Y. J. Chun, and H. C. So, "Modeling and performance analysis of blockchain-aided secure TDOA localization under random internet-of-vehicle networks," *Signal Process.*, vol. 206, 2023, Art. no. 108904.

[12] H. C. So, Y. T. Chan, and F. K. W. Chan, "Closed-form formulae for time-difference-of-arrival estimation," *IEEE Trans. Signal Process.*, vol. 56, no. 6, pp. 2614–2620, Jun. 2008.

[13] M. Haenggi, *Stochastic Geometry for Wireless Networks*. Cambridge, U.K.: Cambridge Univ. Press, 2013.

[14] P. Bromiley, "Products and convolutions of Gaussian probability density functions," TINA-Vis. Memo, Manchester, U.K., Tech. Rep. 2003-003, 2003.

[15] H. C. So, "Technique for numerical computation of Cramér-Rao bound using MATLAB," 2016. [Online]. Available: https://sigport.org/documents/technique-numerical-computation-cram%C3%A9r-rao-bound-using-matlab

[16] X. Zhang, C. Tepedelenlioğlu, M. Banavar, and A. Spanias, "CRLB for the localization error in the presence of fading," in *Proc. IEEE Int. Conf. Acoust. Speech Signal Process.*, Vancouver, BC, Canada, 2013, pp. 5150–5154.

[17] R. Bellman, *Introduction to Matrix Analysis*. New York, NY, USA: McGraw-Hill, 1960.

[18] M. Sadeghi, F. Behnia, and R. Amiri, "Optimal geometry analysis for elliptic localization in multistatic radars with two transmitters," *IEEE Trans. Aerosp. Electron. Syst.*, vol. 58, no. 1, pp. 697–703, Feb. 2022.

[19] W.-J. Zeng, H. C. So, and A. M. Zoubir, "An l_p-norm minimization approach to time delay estimation in impulsive noise," *Digit. Signal Process.*, vol. 23, 1247–1254, 2013.

[20] R. Barakat, "Probability density functions of sums of sinusoidal waves having nonuniform random phases and random numbers of multipaths," *J. Acoust. Soc. Amer.*, vol. 83, no. 3, pp. 1014–1022, 1988.

[21] W. Liu, X. Zang, Y. Li, and B. Vucetic, "Over-the-air computation systems: Optimization, analysis and scaling laws," *IEEE Trans. Wireless Commun.*, vol. 19, no. 8, pp. 5488–5502, Aug. 2020.